

The metastable phase Ni₂Mo and the initial stages of ordering in NiMo alloys

— [Source link](#) 

S. K. Das, Gareth Thomas

Institutions: University of California, Berkeley

Published on: 16 Jan 1974 - Physica Status Solidi (a) (John Wiley & Sons, Ltd)

Topics: Phase (matter)

Related papers:

- [Short range order in Ni-Mo, Au-Cr, Au-V and Au-Mn alloys](#)☆
- [Electron Diffraction and Electron Microscopic Study of Long- and Short-Range Order in Ni₄Mo and of the Substructure Resulting from Ordering](#)
- [On short range order and micro-domains in the Ni₄Mo system](#)
- [k-Space symmetry rules for order-disorder reactions](#)Regles de symetrie dans l'espace des k pour les transformations ordredesordreSymmetrieregeln im k-Raum für ordnungsübergänge
- [Long range order in Ni₃Mo based ternary alloys—I. Isothermal aging response](#)

Share this paper:    

View more about this paper here: <https://typeset.io/papers/the-metastable-phase-ni2mo-and-the-initial-stages-of-4tajn00hg4>

Lawrence Berkeley National Laboratory

Recent Work

Title

THE METASTABLE PHASE Ni₂Mo AND THE INITIAL STAGES OF ORDERING IN Ni-Mo ALLOYS

Permalink

<https://escholarship.org/uc/item/4nk57070>

Authors

Das, S.K.
Thomas, G.

Publication Date

1973-07-01

THE METASTABLE PHASE Ni_2Mo AND THE INITIAL STAGES
OF ORDERING IN Ni-Mo ALLOYS*

S. K. Das and G. Thomas

RECEIVED
LAWRENCE
BERKELEY LABORATORY

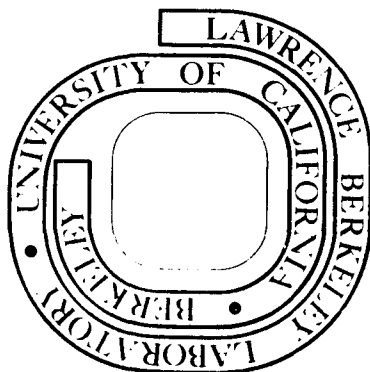
July 1973

LIBRARY AND
DOCUMENTS DIVISION

Prepared for U. S. Atomic Energy Commission
under Contract W-7405-ENG-48

TWO-WEEK LOAN COPY

*This is a Library Circulating Copy
which may be borrowed for two weeks.
For a personal retention copy, call
Tech. Info. Division, Ext. 5545*



DISCLAIMER

This document was prepared as an account of work sponsored by the United States Government. While this document is believed to contain correct information, neither the United States Government nor any agency thereof, nor the Regents of the University of California, nor any of their employees, makes any warranty, express or implied, or assumes any legal responsibility for the accuracy, completeness, or usefulness of any information, apparatus, product, or process disclosed, or represents that its use would not infringe privately owned rights. Reference herein to any specific commercial product, process, or service by its trade name, trademark, manufacturer, or otherwise, does not necessarily constitute or imply its endorsement, recommendation, or favoring by the United States Government or any agency thereof, or the Regents of the University of California. The views and opinions of authors expressed herein do not necessarily state or reflect those of the United States Government or any agency thereof or the Regents of the University of California.

THE METASTABLE PHASE Ni₂Mo AND THE INITIAL STAGES

OF ORDERING IN Ni-Mo ALLOYS *

S. K. Das¹) and G. Thomas

Inorganic Materials Research Division, Lawrence Berkeley Laboratory, and
Department of Materials Science and Engineering, College of Engineering,
University of California, Berkeley, California 94720.

The initial stages of ordering in Ni₃Mo and Ni₄Mo have been investigated by transmission electron microscopy and diffraction. The development of long-range order in Ni₃Mo is associated with decomposition into the two metastable phases Ni₂Mo and Ni₄Mo, which are eventually replaced by the equilibrium Ni₃Mo at a later stage of ordering. Evidence for the presence of metastable Ni₂Mo phase was also found during the early stages of ordering of Ni₄Mo. The presence of the metastable phase Ni₂Mo at Ni₄Mo composition and that of Ni₂Mo and Ni₄Mo at Ni₃Mo composition can be explained in terms of the recent thermodynamic calculations of the ground states of ordered binary alloys by Cahn and his co-workers.

1. Introduction

There have been a number of studies on the ordering of Ni-Mo alloys, particularly on the systems Ni₄Mo [1—9] and Ni₃Mo [10—12]. In the long-range-ordered (lro) state, Ni₄Mo is body-centered

¹) Now in the Physics Division, Argonne National Laboratory, Argonne, Illinois 60439.

tetragonal and Ni_3Mo has an orthorhombic structure; and both are disordered fcc at high temperature in the single-phase region. On fast quenching from the single-phase region, the decomposition can be suppressed and both the alloys exhibit diffuse short-range order (sro), scattering peaks at $\{1\frac{1}{2}0\}$ position of the fcc reciprocal lattice. In a recent study [13] of the sro state of Ni_4Mo and Ni_3Mo , it was found that both of these alloys are similar in the quenched state and contain weak superlattice reflections corresponding to Ni_4Mo and Ni_2Mo superstructures in addition to the $\{1\frac{1}{2}0\}$ spots. Thus, one may expect these two alloys to behave similarly at the very early stages of the development of lro. Yamamoto et al. [10], who quenched the alloy Ni_3Mo from high temperature single phase region and then allowed it to age, reported that it initially decomposed to Ni_2Mo and then Ni_4Mo precipitated and that these two phases coexist for some time. On prolonged aging these are subsequently replaced by the equilibrium Ni_3Mo phase. In the studies [4—8] on the development of lro in Ni_4Mo , on the other hand, the formation of metastable Ni_2Mo phase has never been reported. Thus, it is not clear why the metastable Ni_2Mo phase is observed in stoichiometric Ni_3Mo but not at Ni_4Mo composition, even though both of them show weak Ni_2Mo superlattice reflections in the as quenched state. The recent calculations of the ground-state structures in ordered binary alloys by Richards [14], by Richards and Cahn [15], and by Allen and Cahn [16] predict that the Ni_2Mo phase may be present in the composition range considered here (20—25 at. % Mo). In view of these results, the initial stages of ordering in both Ni_4Mo and Ni_3Mo were carefully examined by electron microscopy and diffraction, for various isothermal annealing treatments.

The results presented in this paper show that the metastable Ni_2Mo phase can form in very small amounts after appropriate isothermal annealing of the quenched Ni_4Mo . In the alloy Ni_3Mo , both Ni_2Mo and Ni_4Mo phases form simultaneously during the initial stages of ordering. These results provide the experimental evidence for some of the

predictions [14—16] from the calculations of ground-state structures in ordered binary alloys.

2. Crystallography of Ni₂Mo

The crystallographic features of the ordered Ni₄Mo and Ni₃Mo structures have been discussed elsewhere [2, 8, 11] and need not be repeated here. Only a few aspects of the ordered Ni₂Mo structure that are important to this study will be described. The Ni₂Mo phase does not occur in the Ni-Mo phase diagram [17] at stoichiometric composition and has been observed only as a metastable phase. The atomic arrangement has been found [10] to be isomorphous with ordered Pt₂Mo, and Fig. 1(a) shows the body-centered orthorhombic unit cell; the dotted line outlines the fcc unit cell. The relationships between the disordered fcc lattice (α) and the ordered orthorhombic Ni₂Mo lattice are

$$\begin{aligned} [100]_{\text{Ni}_2\text{Mo}} & \parallel [110]_{\alpha} , \\ [010]_{\text{Ni}_2\text{Mo}} & \parallel [\bar{1}10]_{\alpha} , \\ [001]_{\text{Ni}_2\text{Mo}} & \parallel [001]_{\alpha} . \end{aligned}$$

Figure 1b shows the projection of atoms on the (001) plane²); the dotted line outlines the orthorhombic Ni₂Mo lattice and the open circles represent the projection of atoms on a/2 layer above. This structure can be described by the stacking of atoms on either {420} or {220} planes where every third plane contains all Mo and in between all Ni atoms. Thus, the reciprocal lattice of the ordered structure can be constructed from the original fcc lattice, where the superlattice reflections will appear at every $\frac{1}{3} \langle 220 \rangle$ or $\frac{1}{3} \langle 420 \rangle$ reciprocal lattice vectors. This gives rise to six orientation variants of Ni₂Mo corresponding to six variants of {220} because of the two-fold degeneracy associated with stacking on {420} planes. The

²) Unless otherwise specified, the indices refer to the fcc lattice.

reciprocal lattice of ordered Ni_4Mo (D1a) can be constructed in a similar way where the superlattice reflections appear at every $\frac{1}{5} \langle 420 \rangle$ fcc reciprocal lattice vector.

3. Experimental Procedure

The alloys Ni_4Mo and Ni_3Mo were prepared by melting together the required proportions of high-purity (99.99%) Ni and Mo in an arc furnace, back filled with argon. The alloys were melted at least six times, and after each melt the ingot was cut into small pieces and the pieces were intermixed in order to obtain a homogeneous composition. The ingots were encapsulated in quartz tubes in vacuum and were homogenized at temperatures of 1200°C and 1270°C for Ni_4Mo and Ni_3Mo , respectively. The ingots were quenched into water and then cold rolled to 6-mil strips with intermediate anneals. The foils were then finally homogenized in an inert atmosphere and quenched directly into iced brine and subsequently aged. The compositions of the homogenized alloy ingots were 19.7 at %Mo and 25.1 at %Mo for Ni_4Mo and Ni_3Mo , respectively.

The thin foils suitable for transmission electron microscopy were prepared in two stages. The 6-mil foils were first electrolytically thinned to 1–2 mils by the window technique, in which a solution containing 396 cc ethylene glycol, 57 cc perchloric acid, 57 cc hydrofluoric acid, and 27 cc distilled water was used. The temperature of the solution was maintained at 10°C and the applied voltage was 9–11 V. From these 1–2-mil foils, 2.3-mm disks were punched out and were finally jet polished in an electrolyte containing two parts of sulphuric acid and one part water, with the total current kept below 10 mA. The foils were examined in a Siemens Elmiskop IA operated at 100kV.

4. Results

4.1 Ni₃Mo

The isothermal aging studies of Ni₃Mo were carried out at 650°C and all the results to be described below correspond to various aging times at this temperature. The choice of this temperature is based on previous studies on Ni₄Mo [8], which indicate that aging at 650°C is associated with some interesting diffraction effects at the initial stages whereas the ordering reaction at high temperatures (~750°C) is extremely fast and these diffraction effects are missed altogether. Yamamoto et al. [10] aged Ni₃Mo samples at 860°C, which is rather high.

Figure 2A shows a [001] diffraction pattern obtained after aging for 4 h. The pattern consists of fundamental fcc spots and superlattice reflections from both Ni₂Mo and Ni₄Mo phases as indexed in Fig. 2C. Some of the fundamental fcc spots in Fig. 2A have also been indexed. The Ni₂Mo reflections (marked M) appear to be arced towards the neighboring Ni₄Mo reflections (marked N) the main direction of streaking is $\langle 110 \rangle$, whereas the Ni₄Mo reflections are streaked in $\langle 210 \rangle$ directions. The streaking of Ni₄Mo spots after 4 h of aging (Fig. 2A) is similar to that observed by Okamoto and Thomas [8] in Ni₄Mo after 5–10 min of aging at the same temperature; thus Ni₃Mo seems to decompose more slowly than Ni₄Mo at 650°C. There also appears to be some intensity near the $\{1\frac{1}{2}0\}$ positions (marked by arrows), especially along $\langle 100 \rangle$ directions. This intensity is not due to the presence of $\{1\frac{1}{2}0\}$ spots (as is shown by the fact that they do not lie precisely at $\{1\frac{1}{2}0\}$ positions) but arise from the relrods from the other two Ni₄Mo spots that are also streaked in $\langle 210 \rangle$ directions and lie at positions $\frac{1}{10}[002]$ above and below this [001] reciprocal lattice section. Thus, they extend from the $\{1\frac{1}{2}0\}$ position to

the projection of the Ni_4Mo spots, along $\langle 100 \rangle$ directions.

On further aging the Ni_4Mo spots (marked N) become rounded as can be seen in Fig. 2B, whereas the Ni_2Mo spots (marked M) are still spread into arcs. The previous study on Ni_4Mo [8] has shown that the streaking of Ni_4Mo superlattice spots in $\langle 210 \rangle$ directions is not a shape factor effect because the streaking is asymmetrical and the dark field images show equiaxed domains. This streaking of Ni_4Mo spots in $\langle 210 \rangle$ directions was explained [8] to be due to the presence of nonconservative APB's on $\{420\}$ planes. If the APB's are spaced periodically then one would observe satellites; but if the spacing is irregular, these satellites will be broadened into streaks. On aging for longer times, these nonconservative APB's (which have a relatively higher energy than the conservative APB's) are eliminated and the streaks will disappear as seen in Fig. 2B. However, some of them may still remain and it will be seen later that they give rise to very weak streaks. Although the Ni_4Mo spots are not streaked after aging for 49 h (Fig. 2B) the Ni_2Mo spots are still streaked. This makes it doubtful whether an explanation based on APB's, similar to that of Ni_4Mo can be applied to Ni_2Mo or not. A detailed explanation will be given later in this section.

In order to see the actual reason for the arcing of Ni_2Mo spots and to determine their true shape, several other reciprocal lattice sections were examined after various aging treatments. Figures 3 and 4 show $[\bar{1}20]$ and $[121]$ reciprocal lattice sections, respectively. It can be seen from Fig 3A that the Ni_2Mo spots (as indexed in Fig. 3C) are streaked along the $\langle 210 \rangle$ direction and not along $\langle 110 \rangle$ as was apparent from the $[001]$ pattern. A dark field micrograph of the Ni_2Mo spot [as shown by the position of the objective aperture in Fig. 3A] reveals that the Ni_2Mo domains have a plate-like shape forming on (420) planes. Thus, the streaking of Ni_2Mo spots in $\langle 210 \rangle$ directions is a true shape-factor effect due to plate-like domains. The $[\bar{1}20]$ diffraction pattern in Fig 3A also contains some

additional rods from the Ni_4Mo spots whose positions are shown in Fig. 3C by open squares. Their intensities are fairly strong because they lie very close to this section and are still elongated.

The $[\bar{1}21]$ sections (Fig. 4) further confirm that the Ni_2Mo spots are streaked along $\langle 210 \rangle$ directions. Figure 4A shows the diffraction pattern after 4 h of aging. Each of the three variants of Ni_2Mo that are present is streaked in a different $\langle 210 \rangle$ direction. Since the variant marked by open triangles [Fig. 4B] is streaked in a $\langle 210 \rangle$ direction that intersects the $[\bar{1}21]$ section at an angle, this spot appears slightly elliptical [Fig. 4A]. In fact, the streaks in the $\langle 210 \rangle$ directions appear to extend continuously from one reciprocal lattice point to another [Fig. 4A] with maxima at Ni_2Mo and Ni_4Mo positions.

Now after establishing that the Ni_2Mo spots are streaked in $\langle 210 \rangle$ directions as a result of a shape-factor effect, we can examine why in the $[001]$ diffraction pattern the streaking appears to be along $\langle 110 \rangle$. As described above (Fig. 1), the Ni_2Mo structure, for example, stacking on (420) and (240) planes gives rise to the same variant of Ni_2Mo (Spot A in Fig. 2C). Thus if plate-like Ni_2Mo domains form with equal probability on (420) and (240) planes, the Ni_2Mo spot at A will be streaked both in $[420]$ and $[240]$ directions, as shown by the thick lines (Fig. 2C). Since these two directions are fairly close to each other and the streaks are fairly wide, these two streaks are not discernible from each other in a $[001]$ orientation and give rise to an apparent streak in the $\langle 110 \rangle$ direction and an arcing towards the neighboring Ni_4Mo spots. However, the $[\bar{1}20]$ section contains only one direction of the streak as can be seen from the trace in Fig. 2C and it is possible to see that the Ni_2Mo spots are, in fact, streaked in $\langle 210 \rangle$ directions. Similar is the case with $[121]$ orientation whose trace on $[001]$ section is the same as that of $[\bar{1}20]$. These results show that it is the same as that of $[\bar{1}20]$. These results show that it is absolutely necessary to examine certain particular reciprocal lattice sections such

as $[\bar{1}20]$ and $[121]$ in order to reveal the origin of the diffraction effects associated with Ni_2Mo spots, or else erroneous conclusions may be drawn. It may be mentioned that Yamamoto et al. [10] reported plate-like Ni_2Mo precipitates to form in Ni_3Mo on $\{110\}$ planes after annealing for 30 min at 860°C . It is not clear whether there is an error in their analysis, as they did not report any evidence of streaks, or the difference may be due to different isothermal annealing treatments.

The Ni_2Mo and Ni_4Mo phases coexist for a long time (up to about 160 h of aging), but after about 250 h they disappear and the equilibrium Ni_3Mo phase appears [18]. Thus, the stoichiometric Ni_3Mo first decomposes to two metastable phases Ni_2Mo and Ni_4Mo . In the initial stages of decomposition the Ni_2Mo phase forms plate-like domains on $\{420\}$ planes that give rise to pronounced streaking in the diffraction pattern, whereas the Ni_4Mo phase does not form plate-like domains but still shows streaking in the diffraction patterns in $\langle 210 \rangle$ directions. At an intermediate stage of aging, the streaking of Ni_4Mo spots disappear whereas those of Ni_2Mo spots remain. On prolonged aging, the metastable phases Ni_2Mo and Ni_4Mo are both replaced by the equilibrium Ni_3Mo .

4.2 Ni_4Mo

As in the case of Ni_3Mo , the isothermal aging treatments for the Ni_4Mo alloy were carried out at 650°C for various times from 5 min to 50 h; but only some typical results pertinent to this study will be described. Figure 5 shows a $[001]$ diffraction pattern obtained after aging for 8 h. This pattern contains two variants of the Ni_4Mo superlattice reflections (which are indexed in Fig. 2C). In addition to the Ni_4Mo superlattice reflections, there are also weak Ni_2Mo superlattice reflections (marked by the single arrows). This pattern is very similar to the pattern obtained from Ni_3Mo (Fig. 2 B), except that Ni_2Mo reflections are very

weak. Much as in the case of Ni_3Mo , the weak Ni_2Mo spots are arced towards the neighboring Ni_4Mo spots. There are also some retrods (marked by double arrows) from the Ni_4Mo spots that lie $\frac{1}{10}[002]$ above and below this reciprocal lattice section.

In order to confirm the presence of a Ni_2Mo phase, some other reciprocal lattice sections were also examined. Figure 6 shows a $[121]$ diffraction pattern and the corresponding microstructure obtained after aging for 8 h. In Fig. 6A, the typical tweed contrast can be seen and the direction of the tweed striations coincides with the trace of the $(10\bar{1})$ plane. Figure 6B is the dark-field micrograph of one variant of the Ni_4Mo superlattice reflection (marked b in Fig. 6C) and shows an alignment of the domains more or less in the direction of the tweed striations. Some typical areas are marked by arrows. These results show that the ordered domains are not in a random array of particles but are arranged in some ordered fashion in three dimensions. At this stage it is not possible to describe further the exact nature of the ordered array.

The $[121]$ diffraction pattern in Fig. 6C clearly shows the presence of Ni_2Mo superlattice reflections of different variants that are streaked in different $\langle 210 \rangle$ directions. The indexing of this pattern is identical to that in Fig. 4B and some of the Ni_2Mo spots are marked by single arrows. Here the $\langle 210 \rangle$ streaks are elongated continuously from one superlattice reflection to another, with maxima at the Ni_2Mo positions (marked by the single arrows), similar to the weak $\langle 210 \rangle$ streaks observed in Ni_3Mo (Fig. 4). This means that the Ni_2Mo phase exists as very thin platelets whose thickness is of the order of a unit cell. There are also some weak double diffraction spots present (marked by double arrows), from the different variants of the Ni_4Mo reflections. It must be pointed out that the detection of these weak spots depends very much on the exposure time, foil contamination, etc. In relatively thicker foils, these weak spots are difficult to detect at 100 kV because of the presence of the Kikuchi lines or bands. The presence of the Ni_2Mo superlattice reflections was also

detected [18] for aging times up to 24 h but these Ni_2Mo peaks in the $\langle 210 \rangle$ streaks did not grow into strong superlattice reflections. The fact that these $\langle 210 \rangle$ streaks through the Ni_2Mo reflections do not vanish even after aging for 24 h implies that the Ni_2Mo phase does not grow beyond a thickness of a few atom layers. It will be shown later in Section 4 that this monolayer of Ni_2Mo phase arises from the presence of nonconservative APB's on $\{420\}$ planes in Ni_4Mo phase.

For aging treatments beyond 24 h, the structure is dominated by the heterogeneous reaction at the grain boundaries. Figure 7 shows an example. The heterogeneous reaction starts at the grain boundary and advances into the next grain B. The structure inside the heterogeneous component A contains a dense array of dislocations and APB's.

A similar heterogeneous reaction mode has been observed in Ni_2V [19] and it has been found that this heterogeneous reaction at the grain boundary is the predominant decomposition mode at lower temperatures.

The important observation on Ni_4Mo is the presence of weak superlattice reflections corresponding to Ni_2Mo phase. The pronounced streaking of Ni_2Mo reflections in $\langle 210 \rangle$ directions implies that this phase arises from the presence of nonconservative APB's on $\{420\}$ planes of Ni_4Mo domains. At a later stage of aging, heterogeneous reaction starts at the grain boundary and this heterogeneously nucleated phase migrates from the grain boundary into the whole grain. No Ni_2Mo phase is present in the final equilibrium Ni_4Mo phase.

5. Discussion

The results described above clearly indicate that the Ni_2Mo can form as a metastable phase in the Ni-Mo alloy in the composition range 20—25 at % Mo, although this phase does not appear in the equilibrium phase diagram [17,18]. First we will discuss some thermodynamic reasons

for the formation of the metastable Ni_2Mo and Ni_4Mo phases at stoichiometric Ni_3Mo compositions and then discuss some structural considerations.

Recently Richards [14], Richards and Cahn [15] have outlined a procedure for deriving the ground state of binary ordering alloys as a function of composition and the first and second nearest-neighbor interaction parameters V_1 and V_2 . The ground state for a given basic crystal structure, composition, and V_i is the state that has lowest configurational energy. If there are total N atoms arranged on a lattice and C is the fraction of B atoms (in the present case it is fraction of Mo atoms), the energy of mixing E can be written [14] as follows:

$$\text{For } \underline{\text{Ni}_4\text{Mo}}, \frac{E}{NV_1} = -\frac{3}{5} - 3C - 2C \left(\frac{V_2}{V_1} \right) \text{ for } 0.2 \leq C \leq 0.3 \quad (1)$$

$$\frac{E}{NV_1} = -\frac{3}{5} - 3C - \frac{3}{5} \left(\frac{V_2}{V_1} \right) \text{ for } 0.3 \leq C \leq 0.4 \quad (2)$$

$$\text{For } \underline{\text{Ni}_2\text{Mo}}, \frac{E}{NV_1} = -\left(3C + \frac{1}{2}\right) - 3C \left(\frac{V_2}{V_1} \right) \text{ for } 0.167 \leq C \leq 0.33 \quad (3)$$

$$\text{For } \underline{\text{DO}_{22}}, \frac{E}{NV_1} = \left(-3C + \frac{3}{4}\right) - \frac{V_2}{V_1} \left(3C - \frac{1}{2}\right) \text{ for } 0.25 \leq C \leq 0.375 \quad (4)$$

By use of these equations, the energy of mixing was calculated for the three structures for different values of the ratios V_2/V_1 . From Fig. 8, which shows the results of such a calculation for $V_2/V_1 = 0.4$, it can be seen that the configurational energies of the Ni_4Mo , Ni_2Mo , and DO_{22} structures are nearly equal; and at 25 at % solute those of Ni_2Mo and Ni_4Mo are almost identical. Because of the approximations involved in Richards [14] calculations in arriving at the configurational energies, there may be an error of 10—15% in the estimated values. Hence it is rather

difficult to say which of the three structures DO_{22} , Ni_2Mo , or Ni_4Mo has the lowest energy. All we can really say is that the energies of the three structures are close to one another. The most recent calculation by Allen and Cahn [16], who used a cluster method, indeed show that for $V_1 > 0$ and $0 \leq (V_2/V_1) \leq 0.5$ the ground-state structure is a polyphase mixture of A_5B (which is same as Ni_2Mo at a different stoichiometry see Richards [14]), Ni_4Mo , and DO_{22} structures. According to them the energy of mixing of the polyphase mixture of the three structures Ni_2Mo , Ni_4Mo , and DO_{22} can be written as

$$\frac{E}{NV_1} = -6C + 3C\left(\frac{V_2}{V_1}\right) - \left(\frac{V_2}{V_1}\right) \text{ for } 0.167 \leq C \leq 0.25. \quad (5)$$

The configuration energy obtained from this equation is also shown in Fig. 8 for $V_2/V_1 = 0.4$. It may be noted that these values are very close to those calculated from Richards' equations. In these calculations, the value of $V_2/V_1 = 0.4$ has been chosen as an example because in our earlier [13] computation of diffuse sro scattering maps for Ni_3Mo by use of the Clapp-Moss theory [20] it was seen that the ratio $V_2/V_1 = 0.4$ gave reasonable agreement with the experimental diffuse-scattering results.

The experimental results presented in the present paper are in qualitative agreement with the above thermodynamic predictions. At the same time, the thermodynamic calculations plausibly explain why Ni_2Mo and Ni_4Mo phases form during the decomposition of Ni_3Mo and also explain the presence of Ni_2Mo phase at Ni_4Mo composition. Now since thermodynamic calculations predict that the configurational energy for the DO_{22} structure should be similar to those for Ni_2Mo and Ni_4Mo (Fig. 8), one may question why this structure is not observed as a metastable phase. It has been shown earlier [8, 13] that the presence of $\{1\frac{1}{2}0\}$ sro spots in Ni-Mo

alloys can be interpreted as due to imperfectly ordered microdomains based on DO_{22} structure. The microdomains observed in the dark-field micrographs of $\{1\frac{1}{2}0\}$ spots in Ni_4Mo [2, 8] and in Ni_3Mo [13] at the very early stages of ordering predominantly consist of imperfectly ordered regions of DO_{22} . The presence of weak Ni_2Mo and Ni_4Mo superlattice reflection shows that some microdomains with these structures also coexist [13]. Thus these experimental results are in agreement with the thermodynamic predictions [14-16]. On further aging of the quenched Ni-Mo alloys, local composition fluctuations may continuously transform the DO_{22} regions to Ni_2Mo and Ni_4Mo that have similar energies. In the case of Ni_3Mo , the stoichiometry is easily balanced if both Ni_2Mo and Ni_4Mo form simultaneously side by side.

Apart from the thermodynamic reasoning, a close examination of the Ni_2Mo and Ni_4Mo structures shows why Ni_2Mo can be present in Ni_4Mo . It has been shown earlier [8] that the DO_{22} structure can be formed from $D1a$ by introducing APBs of the nonconservative type. In a similar manner, Ni_2Mo structure can also be created from Ni_4Mo and vice versa. Figure 9 shows an example in which an APB of the type $(420)\frac{1}{2}[\bar{1}01]$ has been introduced on the (420) plane in the fully ordered $D1a$ structure. The notations used are the same as those in Fig. 1. The introduction of such an APB is equivalent to removing two layers of {420} planes containing Ni atoms exclusively. A comparison of the area in the vicinity of the APB with Fig. 1 shows that the structure locally transforms to Ni_2Mo type, as if a platelet of thickness $3d_{420}$ is formed on the (420) plane. Some of these local regions may act as nuclei for Ni_2Mo phase; some may grow and some may stay as platelets. The observation of the weak $\langle 210 \rangle$ streaks extending from one superlattice reflection to another with a maximum at the Ni_2Mo position in Fig. 4A for Ni_3Mo and in Figs. 5 and 6C for Ni_4Mo can now be explained as being due to these thin plate-like Ni_2Mo regions formed on {420} planes.

6. Conclusions

- 1) During the initial stages of ordering of Ni_3Mo , both Ni_2Mo and Ni_4Mo occur as metastable phases. The Ni_2Mo phase forms as plate-like particles on $\{420\}$ planes but Ni_4Mo phase is more or less equiaxed.
- 2) The Ni_2Mo phase also occurs as a metastable phase during ordering of Ni_4Mo , but its volume fraction is restricted.
- 3) The experimental results support the thermodynamic predictions that the ground-state structures in Ni-Mo alloys in the composition range 16—25 at % Mo is a polyphase mixture. The thermodynamic calculations explain why Ni_2Mo occurs as a metastable phase during the ordering of Ni-Mo alloys.
- 4) A structural model based on the presence of nonconservative APBs shows that such APBs are nuclei for Ni_2Mo phase in stoichiometric Ni_4Mo .

Acknowledgements

This work was supported by the U.S. Atomic Energy Commission through the Inorganic Materials Research Division, Lawrence Berkeley Laboratory, University of California, Berkeley, California. The authors are grateful to Dr. P. R. Okamoto for his cooperation and many helpful discussions during the course of this work.

References

- [1] J. E. SPRUIELL and E. E. STANSBURY, J. Phys. Chem. Solids 26, 811 (1965).
- [2] E. RUEDL, P. DELAVIGNETTE, and S. AMELINCKX, phys. stat. sol. 28, 305 (1968).
- [3] B. G. LeFEVRE, A. G. GUY, and R. W. GOULD, Trans. AIME 242, 788 (1968).
- [4] T. SABURI, K. KOMATSU, and S. NENNO, Phil. Mag. 20, 1091 (1969).
- [5] W. B. SNYDER and C. R. BROOKS, in: Ordered Alloys, Proceedings of Third Bolton Landing Conference, September 1969, B. H. KEAR, C. T. SIMS, N. S. STOLOFF, and J. H. WESTROOK (Eds.), Claitor's Publishing Division, Baton Rouge, Louisiana, 1970 (p. 275).
- [6] B. CHAKRAVARTI, E. A. STARKE, B. G. LeFEVRE, J. Mater. Sci. 5, 394 (1970).
- [7] P. R. OKAMOTO and G. THOMAS, Mat. Res. Bull. 6, 45 (1971).
- [8] P. R. OKAMOTO and G. THOMAS, Acta Met. 19, 825 (1971).
- [9] F. LING and E. A. STARKE, Acta Met. 19, 759 (1971).
- [10] M. YAMAMOTO, S. NENNO, T. SABURI, and Y. MIZUTANI, Trans. JIM 11, 120 (1970).
- [11] E. RUEDL and S. AMELINCKX, Mat. Res. Bull. 4, 361 (1969).
- [12] E. RUEDL and S. AMELINCKX, Crystal Lattice Defects 2, 247 (1971).
- [13] S. K. DAS, P. R. OKAMOTO, P. M. J. FISHER, and G. THOMAS, Acta Met., in press.
- [14] M. J. RICHARDS, Sc. D. Thesis, Massachusetts Institute of Technology, Cambridge, 1971.
- [15] M. J. RICHARDS and J. W. CAHN, Acta Met. 19, 1263 (1971).
- [16] S. M. ALLEN and J. W. CAHN, Acta Met. 20, 423 (1972).
- [17] F. A. Shunk, Constitution of Binary Alloys, Second Supplement, McGraw-Hill Book Company, N. Y., 1969 (p. 515).

- [18] S. K. DAS, Ph. D. Thesis, University of California, Berkeley, Lawrence Berkeley Laboratory Report No. LBL 176 (1971).
- [19] L. E. TANNER, *Acta Met.* 20, 1197, (1972).
- [20] P. C. CLAPP and S. C. MOSS, *Phys. Rev.* 171, 754 (1968).

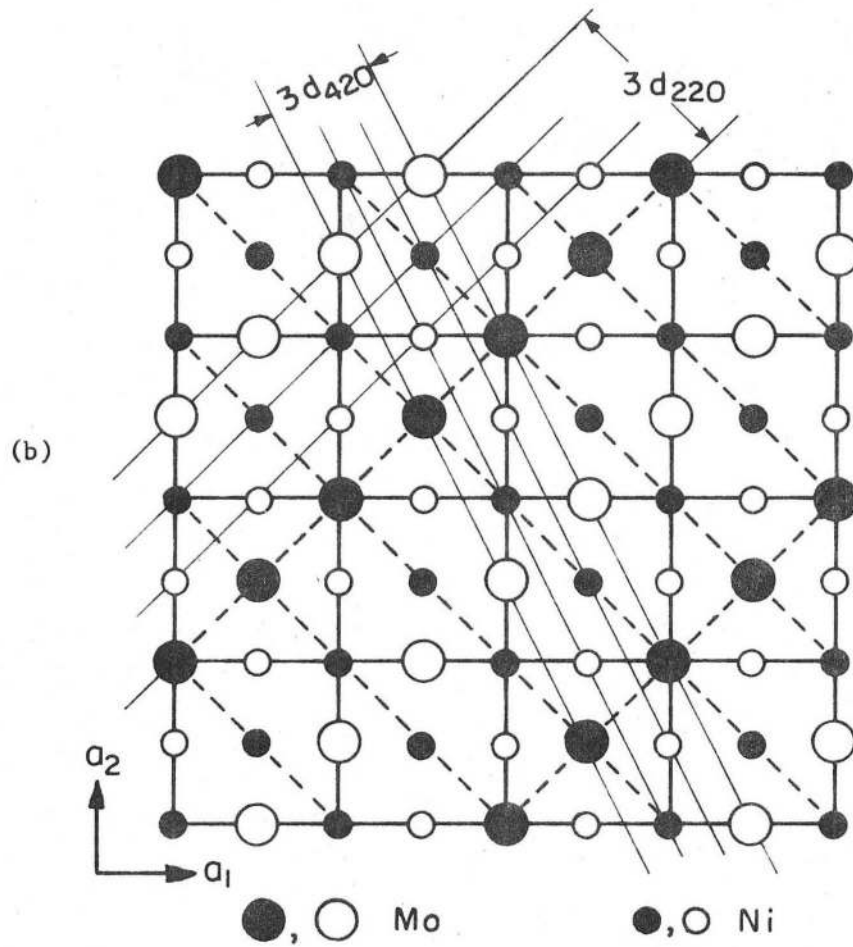
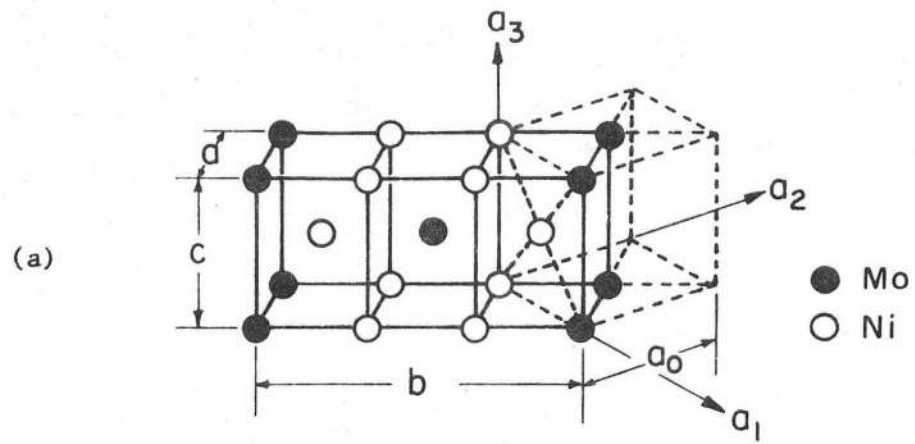
FIGURE CAPTIONS

- Fig. 1. The crystal structure of ordered Ni_2Mo : (a) the orthorhombic unit cell as derived from the original fcc lattice and (b) the atomic packing on the (001) plane.
- Fig. 2. The [001] diffraction patterns from a Ni_3Mo sample. Photographs (A) and (B) were obtained after aging at 650°C for 4 h and 49 h, respectively. The diagram (C) is the indexed pattern. The arrows in (A) point to the relrods corresponding to Ni_4Mo reflections.
- Fig. 3. (A) The $[\bar{1}20]$ diffraction pattern of a Ni_3Mo sample after aging for 49 h at 650°C . (B) Dark field micrograph of Ni_2Mo spot whose position is shown in (A) by the superimposed image of the objective aperture, (C) the indexed $[\bar{1}20]$ pattern.
- Fig. 4. (A) The [121] diffraction pattern of Ni_3Mo sample after aging at 650°C for 4 h. (B) The indexed pattern corresponding to one quadrant of the diffraction pattern in (A).
- Fig. 5. The [001] diffraction pattern of Ni_4Mo sample after aging at 650°C for 8 h. The single black-white arrows point to the weak Ni_2Mo superlattice reflections and the small double arrows point to the relrods from Ni_4Mo reflections.
- Fig. 6. Micrographs of Ni_4Mo sample after aging for 8 h at 650° : (A) bright-field micrograph, (B) dark-field micrograph of Ni_4Mo superlattice spot marked b in the [121] diffraction pattern shown in (C), which corresponds to the area in Fig. 6(A). In (C) the foil has been tilted from that in (A) to obtain a symmetrical diffraction pattern. The single large black-white arrows in (C) point to weak Ni_2Mo superlattice reflections and the small double arrows are double diffraction spots from Ni_4Mo .

Fig. 7. Microstructure of Ni_4Mo after aging for 24 h at 650°C . Note the heterogeneous reaction at the grain boundary.

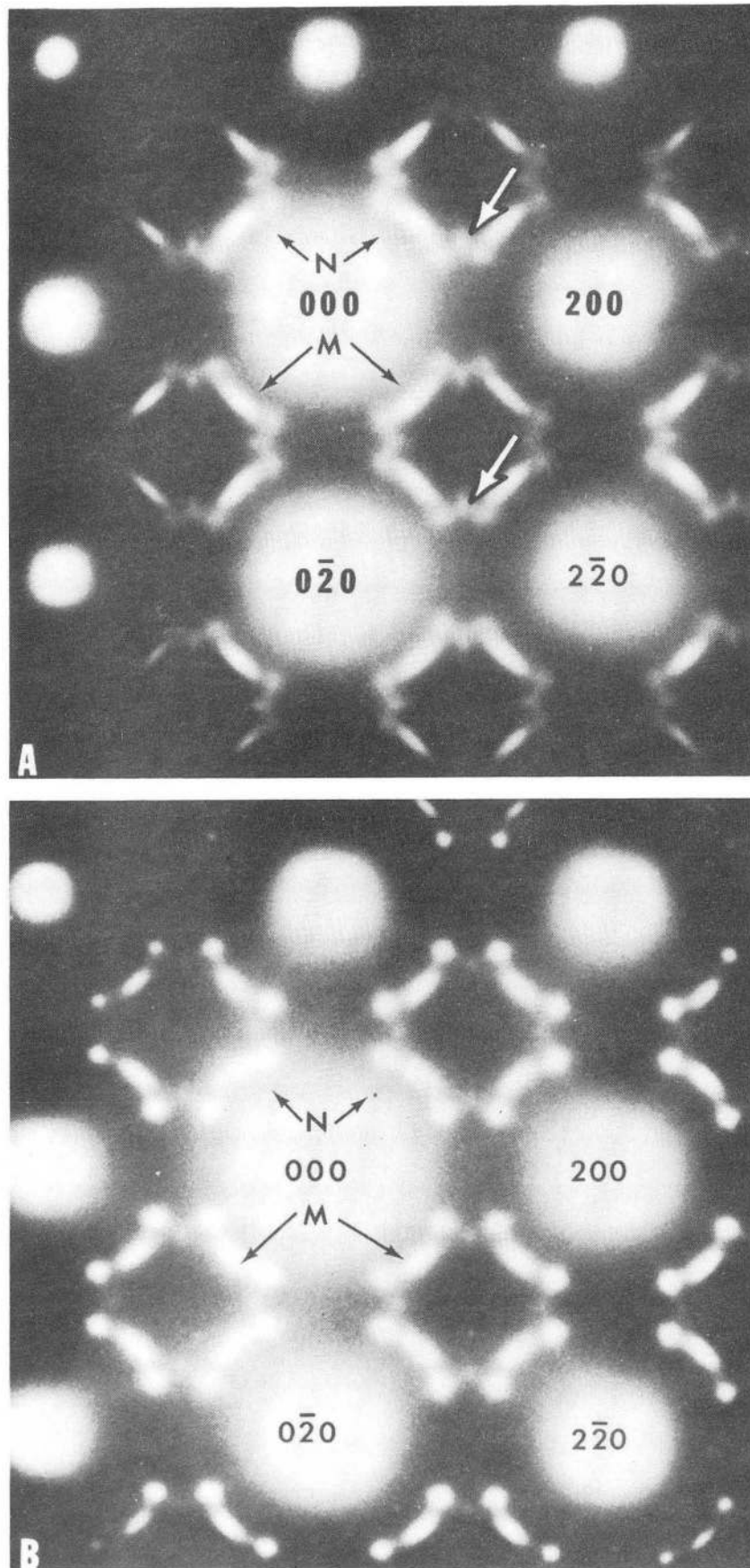
Fig. 8. The theoretical curves for energy of mixing versus composition for DO_{22} , Ni_4Mo and Ni_2Mo structures calculated using $\frac{V_2}{V_1} = 0.4$.

Fig. 9. An APB model showing how the Ni_2Mo structure can be derived from Ni_4Mo structure by introducing a non-conservative APB of the type $(420)\frac{1}{2}[\bar{1}01]$.



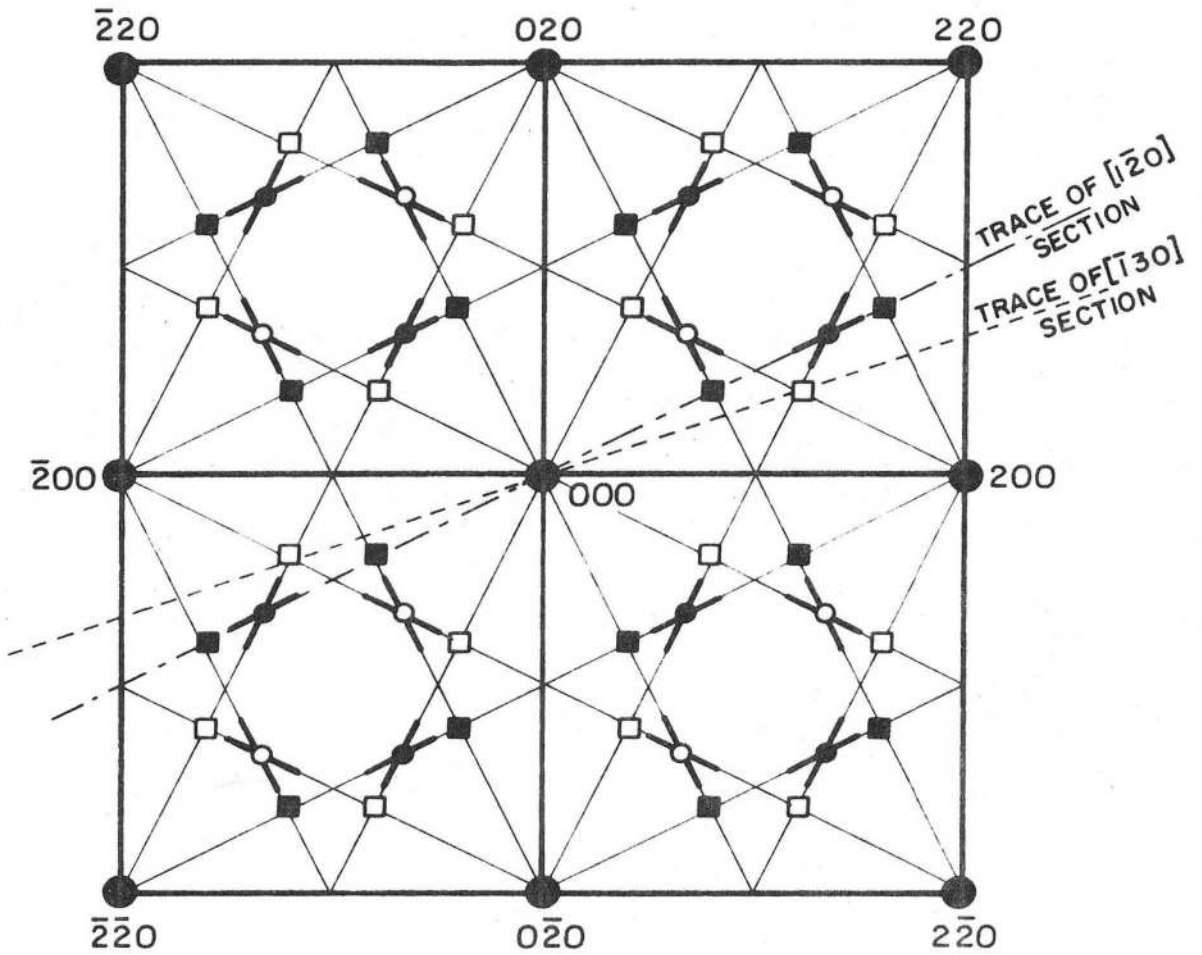
XBL 7110-7335

Fig. 1



XBB 738-4980

Fig. 2



- FUNDAMENTAL FCC SPOTS
- , ● TWO VARIANTS OF Ni_2Mo
- , ■ TWO VARIANTS OF Ni_4Mo

XBL 717-1217

Fig. 2c

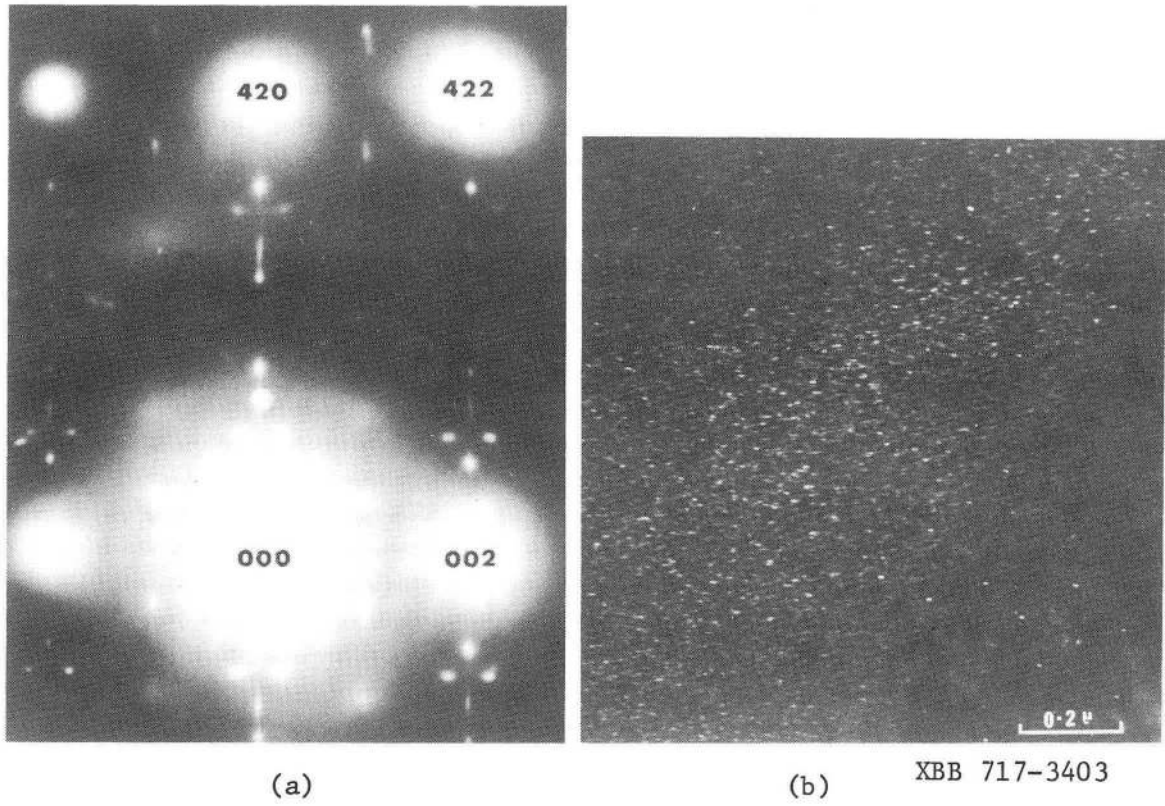
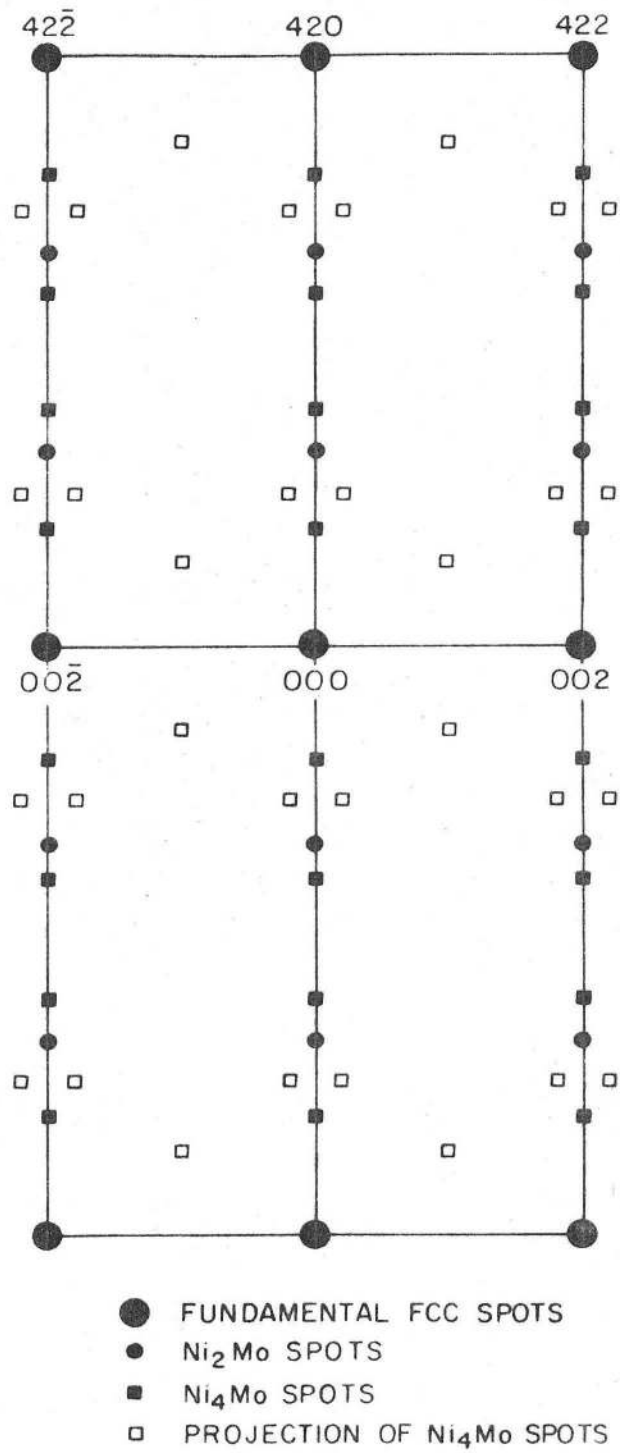
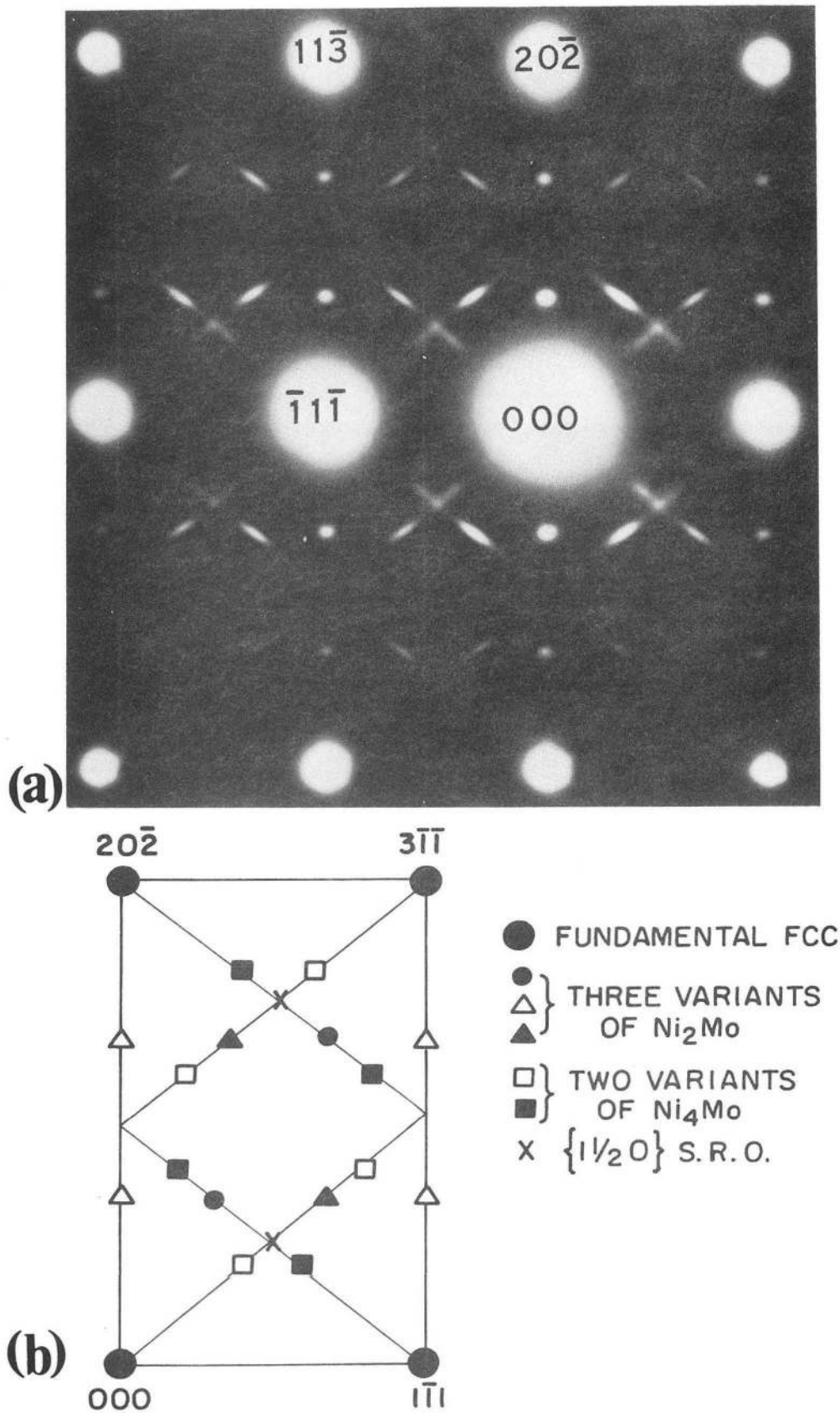


Fig. 3 a,b



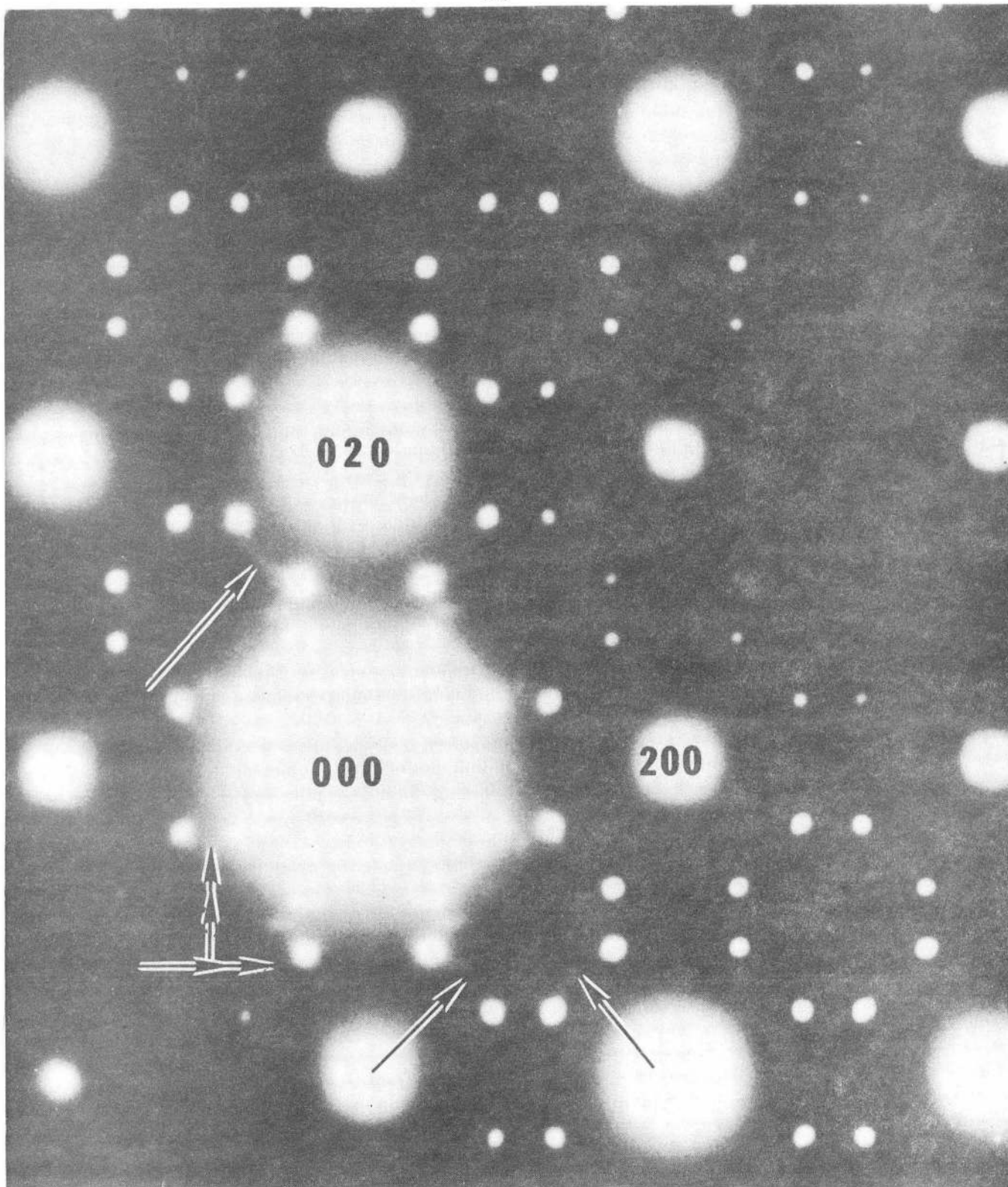
XBL 7110-7337

Fig. 3c



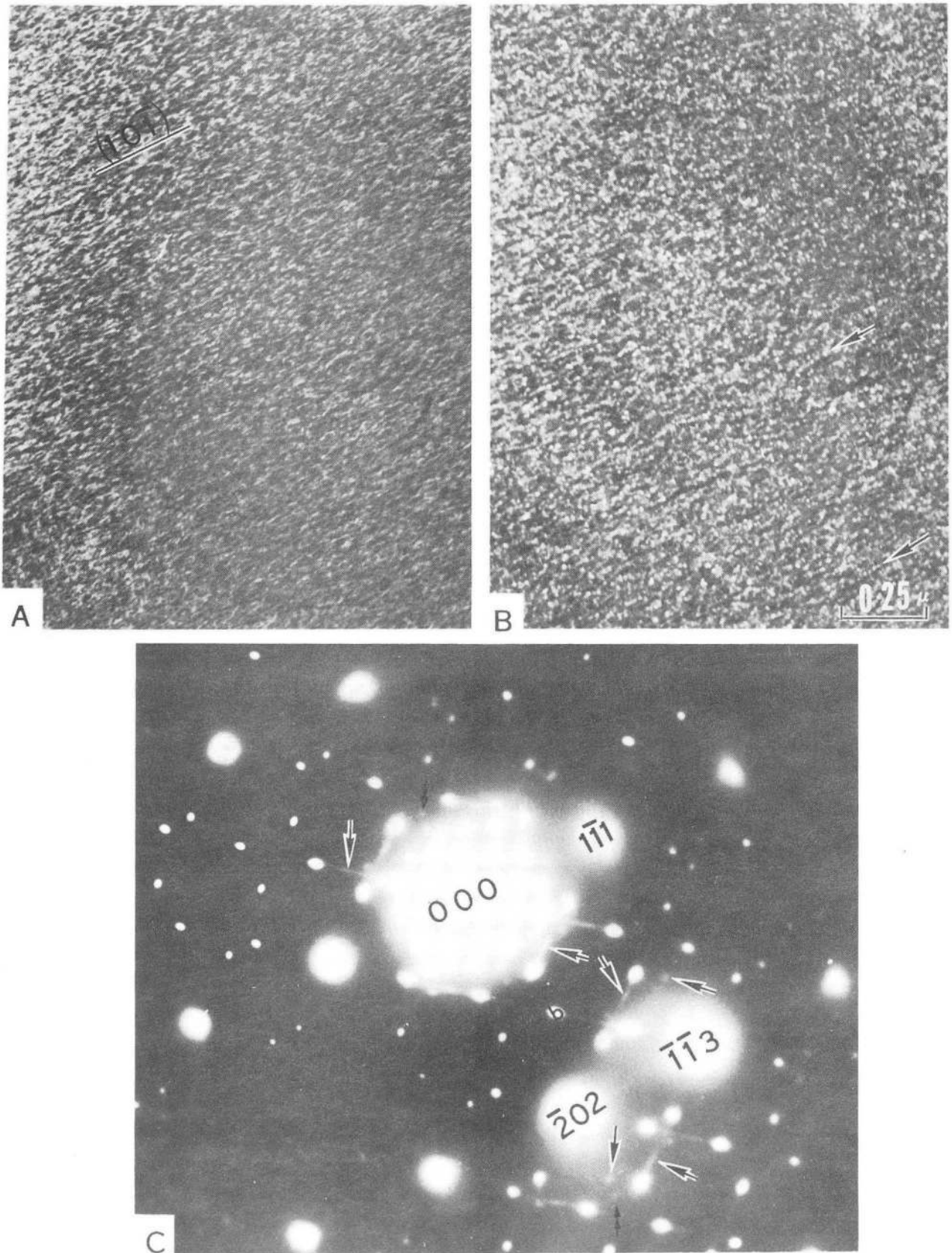
XBB 717-3398

Fig. 4



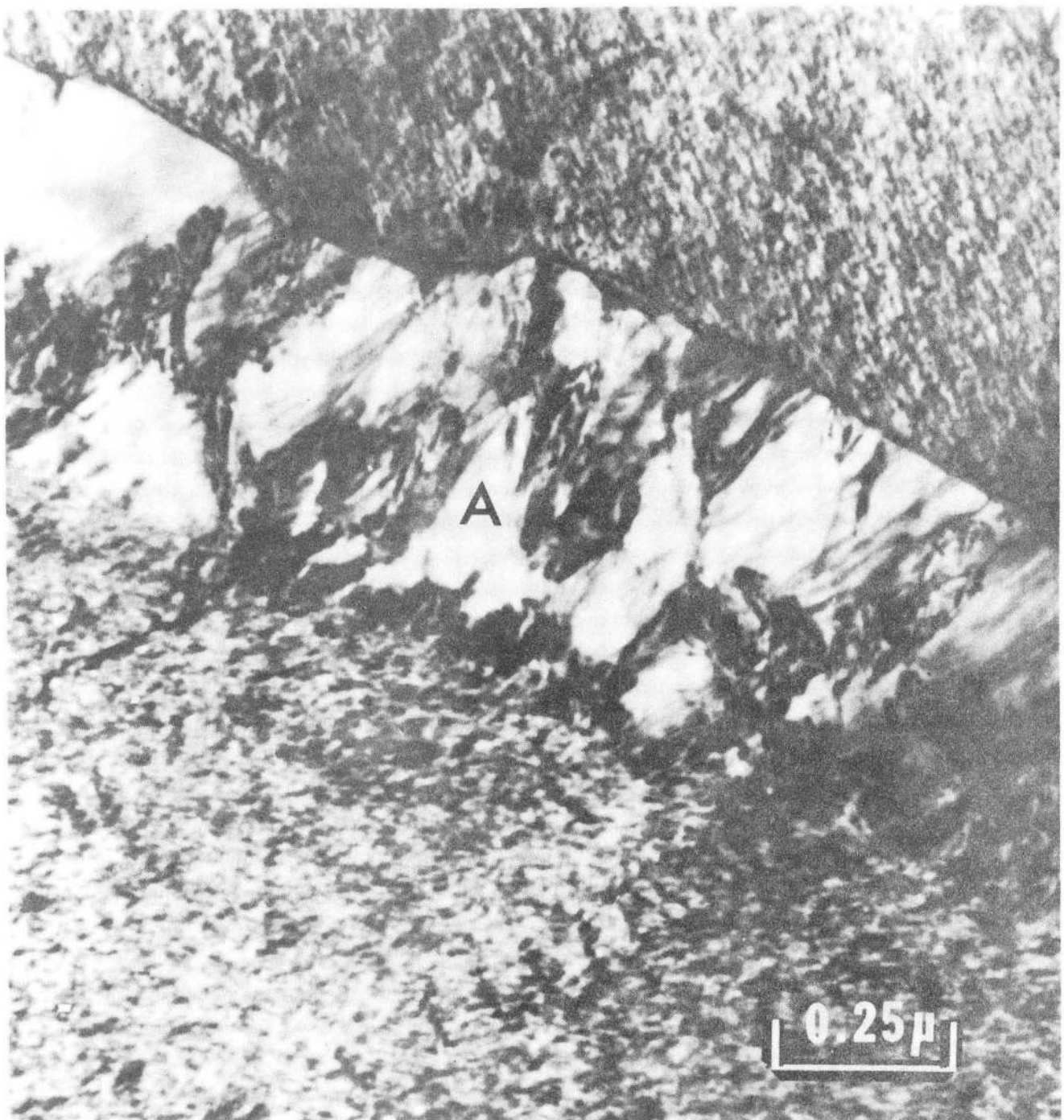
XBB 738-4979

Fig. 5



XBB 738-4981

Fig. 6



XBB 738-4982

Fig. 7

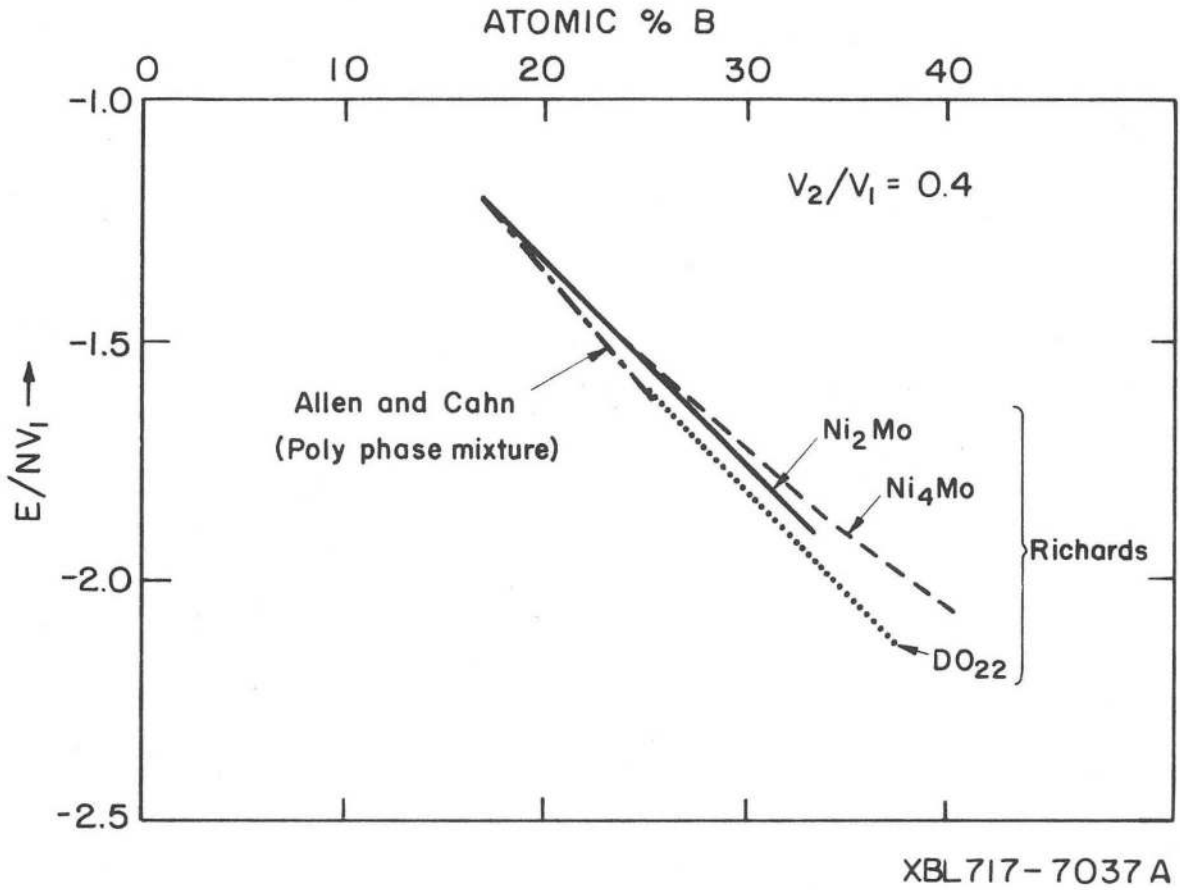
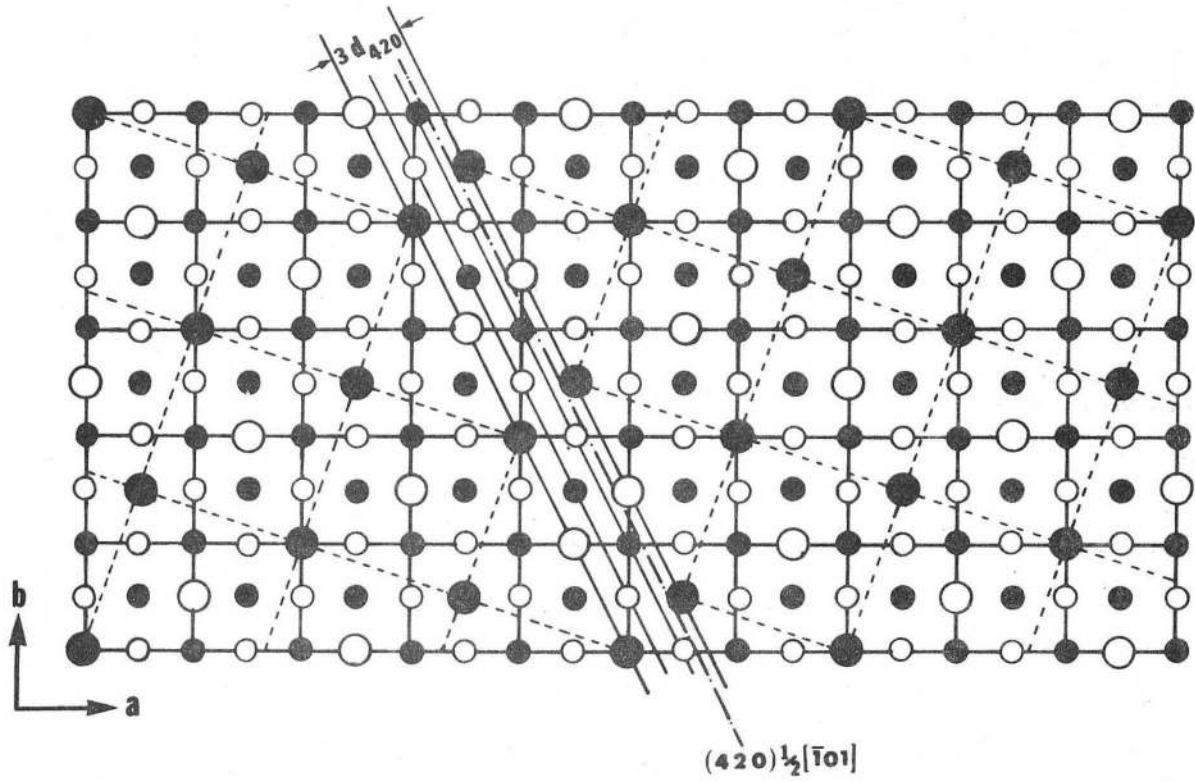


Fig. 8



XBL 717-1216

Fig. 9

LEGAL NOTICE

This report was prepared as an account of work sponsored by the United States Government. Neither the United States nor the United States Atomic Energy Commission, nor any of their employees, nor any of their contractors, subcontractors, or their employees, makes any warranty, express or implied, or assumes any legal liability or responsibility for the accuracy, completeness or usefulness of any information, apparatus, product or process disclosed, or represents that its use would not infringe privately owned rights.

TECHNICAL INFORMATION DIVISION
LAWRENCE BERKELEY LABORATORY
UNIVERSITY OF CALIFORNIA
BERKELEY, CALIFORNIA 94720